Submitted to
J. Chem. Phys.

RECEIVED
LAWRENCE
RADIATION LABORATORY

JAN 30 1973

LIBRARY AND
DOCUMENTS SECTION

LBL-1429 c.2
Preprint

DYNAMICS OF THE O^+-H_2 REACTION. I: REACTIVE SCATTERING OF $O^+(^4S_{3/2})$ AT RELATIVE ENERGIES BELOW 15eV

Keith T. Gillen, Bruce H. Mahan and John S. Winn

~~January 8, 1973~~
December, 1972

Prepared for the U. S. Atomic Energy
Commission under Contract W-7405-ENG-48

TWO-WEEK LOAN COPY

This is a Library Circulating Copy which may be borrowed for two weeks. For a personal retention copy, call Tech. Info. Division, Ext. 5545

LBL-1429 c.2

DISCLAIMER

This document was prepared as an account of work sponsored by the United States Government. While this document is believed to contain correct information, neither the United States Government nor any agency thereof, nor the Regents of the University of California, nor any of their employees, makes any warranty, express or implied, or assumes any legal responsibility for the accuracy, completeness, or usefulness of any information, apparatus, product, or process disclosed, or represents that its use would not infringe privately owned rights. Reference herein to any specific commercial product, process, or service by its trade name, trademark, manufacturer, or otherwise, does not necessarily constitute or imply its endorsement, recommendation, or favoring by the United States Government or any agency thereof, or the Regents of the University of California. The views and opinions of authors expressed herein do not necessarily state or reflect those of the United States Government or any agency thereof or the Regents of the University of California.

Dynamics of the O^+-H_2 Reaction. I: Reactive Scattering of $O^+(^4S_{3/2})$ at Relative Energies Below 15eV.

Keith T. Gillen, Bruce H. Mahan and John S. Winn
Department of Chemistry, and Inorganic Materials Research Division of the Lawrence Berkeley Laboratory, University of California, Berkeley, California.

ABSTRACT

Product velocity vector distributions show that the reaction $O^+(H_2,H)OH^+$ and its isotopic variations proceed from ground state reactants to predominantly electronic ground state products via a direct interaction. Spectator stripping is a prominent feature at the lower relative energies of collision, but the stripping peak is lost at energies where the internal excitation of $OH^+(^3\Sigma^-)$ makes it unstable to dissociation. Production of forward scattered electronically excited OH^+, probably in the $^1\Delta$ state, is observable when the initial relative energy is high enough that $OH^+(^3\Sigma^-)$ formed by spectator stripping is unstable with respect to dissociation. At these relative energies, OH^+ from HD is predominantly scattered into barycentric angles less than 90°, while the OD^+ appears at approximately 90° and larger angles. The propensity for formation of OD^+ at large angles can be understood in terms of general kinematic considerations which apply to collinear collisions.

The reaction of the ground state oxygen ion, $O^+(^4S_{3/2})$, with the hydrogen molecule has received very little attention from kineticists. For the process

$$O^+(^4S_{3/2}) + H_2 \longrightarrow OH^+(^3\Sigma^-) + H \qquad \Delta H = -0.43 \qquad (1)$$

Fehsenfeld et al[1] found a rate constant of 2×10^{-9}cc/sec at 300°K, which is slightly larger than the ion-induced dipole capture rate constant of 1.6×10^{-9}cc/sec. Apparently, no other measurements of the rate constant of this reaction have been made.

The system O^+-H_2 has several features which make it an attractive subject for study by ion beam scattering techniques. Because the masses of the reactants are not too disparate, the kinematic factors which determine resolution in the barycentric system are favorable, particularly for the O^+-D_2 combination. As a triatomic system, it offers at least the possibility of relatively simple interpretation of measured product energy and angular distributions. Moreover, the mass spectrum of H_2O has been well studied, and the appearance potentials of the various fragment ions measured. These data, together with the photoelectron spectrum of H_2O, provide some information about the collision intermediate for conformations close to the equilibrium geometry of H_2O. In particular, it is known from these data that the electronic ground state of H_2O^+ lies 6.12eV below the

reactants,[2] and 5.69eV below the products of reaction (1). This raises the intriguing question of whether this deep potential well is in fact accessible to the reactants, and influences the reaction dynamics.

Useful information concerning this question and the general nature of the potential energy surfaces of the O^+-H_2 system can be gleaned from molecular orbital and electronic state correlation diagrams. Several applications of molecular orbital correlation diagrams to the understanding of ion-molecule reactions have been given by Mahan.[3] Application of the techniques of that paper indicates that $O^+(^4S_{3/2})$ inserted into H_2 gives H_2O^+ in a highly excited electronic configuration, rather than the configuration of the ground state. On the other hand, O^+ and H_2 brought together in a collinear conformation do evolve into the electronic configuration anticipated for ground state OHH^+, which would not be expected to be appreciably lower in energy than either reactants or products. Thus, molecular orbital correlations indicate that O^+ does not insert to form a bound H_2O^+, but rather abstracts H from H_2 by an approximately collinear direct interaction.

While molecular orbital correlations can be very useful, they can become ambiguous whenever orbital energies are not well separated, and the electronic states which

arise from different electronic configurations approach one another and cross as the nuclear conformation is changed. It is therefore more reliable to correlate the electronic <u>states</u> of reactants and products, and examine the consequences of state crossings, should they occur. Figure 1 is a partial correlation diagram for the lower electronic states of the products and reactants of the O^+-H_2 system. A somewhat similar diagram has been presented earlier by Fiquet-Fayard and Guyon.[4] On the left side of the diagram, an approach of the O^+ (or O) along the perpendicular bisector of the H_2(or H_2^+) bond is assumed, and consequently the states are labeled in terms of the symmetry species of the C_{2v} point group. The correlations to the products are indicated for passage through both linear and non-linear HOH^+. On the far right of the diagram, the O^+ is assumed to approach H_2 collinearly, and the intermediate separates to products in the same manner.

Considering first the perpendicular approach of O^+ on H_2, we see that $^4A_2$ is the only state of H_2O^+ that correlates to the ground state reactants $O^+(^4S_u)$ and $H_2(^1\Sigma_g^+)$. Unfortunately, the location of this state on the energy scale is not known for any small O-H distances. However, the $^4A_2$ state is derived from the configuration $(1s)^2(2a_1)^2(1b_2)^1(3a_1)^2(1b_1)^1(4a_1^*)^1$, in which one O-H

bonding $1b_2$ electron has been excited to the O-H antibonding $4a_1^*$ orbital. The $^4A_2$ state should therefore lie well above the known $^2B_2$ state of H_2O^+ which is derived from the configuration $(1s)^2(2a_1)^2(1b_2)^1(3a_1)^2(1b_1)^2$. A rough estimate of the energy of $H_2O^+(^4A_2)$ can be obtained by adding the experimental $^3B_1 \longleftarrow {}^1A_1(4a_1^* \longleftarrow 1b_1)$ excitation energy of neutral[5] H_2O to the energy of the $^2B_2$ state of H_2O^+, and this estimate was used in positioning the $^4A_2$ state in Fig. 1.

The correlations from the states of the C_{2v} H_2O^+ intermediate[6] to the various states of the products are given, but in this intermediate region the positions of the states have at best only qualitative significance. For the products, the energy of OH^+ in the $^3\Sigma^-$ and $^3\pi$ states is well known experimentally,[7] and the position of $OH^+(^1\Delta)$ was established by using the calculations of Cade[8] and Liu and Verhaegen.[9]

If we trace the evolution of the system when $O^+(^4S_{3/2})$ approaches along or close to the perpendicular bisector of the H_2 bond, we see that ground state OH^+ and H can be reached from ground state reactants. However, to do so the system must pass over an energy barrier which may be a few electron volts in height. Collisions with this approximate geometry will not lead to insertion of O^+ into H_2 to form a strongly bound intermediate H_2O^+.

However, since the $^4A_2$ surface does cross the $^2B_2$, $^2A_1$, and $^2B_1$ surfaces, one should consider the possibility that some coupling mechanism exists which would allow the system moving initially on the $^4A_2$ surface to transfer to the strongly bound $^2A_1$, $^2B_1$, or $^2B_2$ states. Examination of the transformation properties of the spin-orbit coupling operator[10] in fact shows that its x,y, and z components, respectively, can couple $^4A_2$ to $^2B_1$, $^2B_2$, and $^2A_1$. Thus in principle, the lower bound states of H_2O^+ are accessible to the reactants, but with a probability which depends on the magnitude of the spin-orbit coupling, the relative velocity of collision, and the angle of intersection between the relevant potential curves, according to the Landau-Zener[11] formula. An approximate evaluation of this probability using the experimental spin-orbit splitting of the oxygen atom, typical velocities, and gross estimates of the angles at which the curves intersect, leads to the conclusion that the system will remain on the $^4A_2$ surface in approximately 99% of all collisions. Nevertheless, the very approximate nature of the calculation requires that we at least entertain the possibility of noticeable transfer to the lower, strongly bound states, with the consequent occurrence of a long-lived collision complex at the lower collision energies, or formation of electronically excited products.

On the far right side of Fig. 1, the correlations between reactants and products are made under the assumption of a linear OHH^+ geometry. In this instance, $O^+(^4S_{3/2})$ and $H_2(^1\Sigma g^+)$ correlate to the ground state products $OH^+(^3\Sigma^-)$ and $H(^2S_{1/2})$ through a $^4\Sigma^-$ surface that does not cross the excited state surfaces. In linear OHH^+, besides the two non-bonding $p\pi$ electrons on the oxygen atom, there occurs the usual three center-three electron σ orbital system in which two electrons occupy a fully bonding three center orbital, and one electron is in an orbital which is antibonding between the end atoms and non-bonding between the end and center atoms. There is no reason to expect a deep potential energy well in this situation, and in fact in neutral systems the three center-three electron situation frequently leads to an activation energy barrier. There can be no appreciable barrier (<0.02eV) in the linear O^+-H_2 system, since the measured reaction rate constant is slightly larger than the ion-induced dipole capture rate. Consequently, collinear or nearly collinear collisions will not involve long-lived complexes, particularly if the relative energy is approximately 1eV or greater.

The tentative conclusions drawn from the correlation diagram are that the $O^+(H_2,H)OH^+$ reaction will proceed by a direct interaction mechanism involving approximately

collinear geometry at the lower collision energies (~1eV). At higher energies, reaction may occur through more nearly perpendicular collision geometries, again with a predominantly direct interaction mechanism. The probability that insertion of ground state O^+ into H_2 to form the ground state or one of the lower excited states of H_2O^+ occurs is finite but probably small, and little if any evidence of a long-lived collision complex is expected. Also, the fraction of products in excited electronic states will probably be small. It is of interest to see whether or not these expectations are consistent with the experimental velocity vector distributions of products and scattered reactants.

EXPERIMENTAL

The instrument used in this work has been described in detail previously.[12] It consists of a magnetic mass spectrometer for preparation of a collimated beam of primary ions of known energy, a scattering cell to contain the target gas, and an ion detection train made up of an electrostatic energy analyzer, a quadrupole mass spectrometer, and an ion counter. The detector components and the exit aperture of the scattering cell are mounted on a rotatable lid, which permits the intensity of scattered ions to be measured at various angles and energies.

Primary ions were extracted from a microwave discharge through oxygen gas. The intensity of the O^+

beam was less than, but comparable to, the intensities of O_2^+ beams that have been extracted from these discharges. This suggests that most of the O^+ comes from ionization of oxygen atoms which are formed first by a variety of discharge processes. The direct dissociative ionization of O_2 to O^+ requires 18.9eV, and in a microwave discharge with an effective electron temperature of 5eV, there are relatively few electrons which have energies in excess of 10eV. Production of O_2^+ ($^4\pi_u$), which requires 16eV, has been shown to be negligible in these discharges.[13] Ionization of the oxygen atom by electrons which have relatively little energy in excess of the lowest ionization energy of 13.6eV should produce predominately ground state $O^+(^4S_{3/2})$, and little if any metastable $O^+(^2D)$ (excitation energy, 3.3eV). In fact, ion beam attenuation experiments of the type described by Turner, et al,[14] and Hughes and Tiernan[15] failed to show any evidence of metastable O^+ in our momentum analyzed beams. Moreover, product intensity scans obtained by using an O^+ beam derived from a microwave discharge through CO_2 had the same appearance as those obtained from discharged O_2. The fraction of excited O^+ formed by electron impact on CO_2 has been shown to be very small.[15] It seems quite certain that the O^+ in our experiments was overwhelmingly in the ground state.

Our experimental results are presented in the form of contour maps of the specific intensity $\bar{I}(\theta,u)$, the intensity of ions per unit velocity space volume

normalized to unit beam strength, scattering gas density, and collision volume. A polar coordinate system is used, with the radial coordinate u representing the speed of the ion relative to the center-of-mass of the target-projectile system, and the angular coordinate θ measured with respect to the original direction of the projectile ion beam. The specific intensity is normalized such that

$$\bar{\sigma} = 2\pi \int_0^{\pi} \sin\theta d\theta \int_0^{\infty} u^2 \bar{I}(\theta, u) du$$

is always proportional to the true total cross section σ. Each contour map is generated from 10-20 scans of the laboratory energy and angular distributions, in each of which 10-20 intensity measurements are made.

RESULTS AND DISCUSSION

More than twenty complete contour maps of the reactively scattered hydroxyl ion were obtained in the relative energy range of 3 to 50eV. We show here representative results which illustrate the most significant features of the product distributions. Figure 2 shows the velocity vector distribution of OH^+ from the $O^+(H_2,H)OH^+$ reaction at an initial relative energy of 4.5eV. The distribution is markedly peaked in the original direction of the primary O^+ beam, forward of the center-of-mass velocity, and is clearly asymmetric about the $\pm 90°$ axis. Another experiment carried out at 3.1eV relative energy

showed very similar features, with forward peaking even more pronounced.

If the reaction were proceeding through a "long-lived" collision complex which existed several rotational periods (only approximately 10^{-13} sec at these energies), a product distribution which was symmetric with respect to the $\pm 90°$ axis would be obtained. The asymmetry evident in the experimental product distributions indicates that the reaction proceeds predominantly by a direct, or short-lived interaction. This conclusion is strengthened by the results of Harris and Leventhal,[16] who found that the OD^+ intensity profiles along the 0°-180° axis in the barycentric system were asymmetric about the centroid velocity even when the initial relative energy was as low as 0.76eV. Potential energy surfaces which contain wells which are deep compared to the initial relative energy of collision have been found[13,17-19] to lead to the symmetric product velocity distribution which is associated with long-lived collision complexes. The absence of any such obvious symmetric components in the product distribution for $O^+(H_2,H)OH^+$ indicates that most collision events do not involve transfer from the $^4A_2$ surface to the strongly bound $^2B_2$, $^2A_1$, or $^2B_1$ states. Instead, the reaction normally proceeds by a direct interaction on the $^4\Sigma^- - {}^4A'' - {}^4A_2$ surface.

The propensity of the O^+-H_2 system to remain on the $^4A_2$-$^4\Sigma^-$ surface in the collision process is related to certain effects observed[4] in the mass spectrum of H_2O. From energetic considerations alone, the appearance potential of $O^+(^4S)$ + H_2 from H_2O should be 18.7eV. However, very little O^+ signal can be detected until the electron energy reaches 26.4eV, the energy necessary to produce $O^+(^2D)$ and two hydrogen atoms or a highly vibrationally excited hydrogen molecule. The O^+ produced by impact of 60eV electrons on water has in fact been shown[15] to consist of 95% metastable excited ions, most probably $O^+(^2D)$. The failure of $O^+(^4S)$ to appear at its expected energy can be easily understood in terms of the correlation diagram, Fig. 1. Removal of an electron from one of the three most weakly bound orbitals of H_2O produces the $^2B_1$, $^2A_1$, and $^2B_2$ states of H_2O^+, none of which correlates to $O^+(^4S)$. Evidently, the mixing of these states with $^4A_2$ by the spin-orbit interaction is not sufficient to permit a strong predissociation to $O^+(^4S)$ and H_2. This is consistent with our conclusion that $O^+(^4S)$ reacts with H_2 predominantly on the $^4A_2$-$^4\Sigma^-$ surface. However, the fact that ionization of H_2O does produce a small amount of $O^+(^4S)$ does indicate that one of the lower states of H_2O^+ (probably $^2B_2$) is slightly predissociated by the $^4A_2$ state. Other consequences of this mixing of doublet and quartet states will become evident in results to be presented later in the paper.

Several other features of the product distribution shown in Fig. 2 are of interest. The intensity peak at 0° occurs very close to the velocity expected from the ideal or spectator stripping model, in which no momentum is imparted to the free H atom product as a result of the reaction. At larger angles, the crater rim or ridge of maximum intensity seems to be on or close to the speed, relative to the center-of-mass, of an OH^+ formed by spectator stripping. That is, the most probable value of Q, the difference between final and initial relative energies seems to be approximately independent of angle. This contrasts quite markedly with the results found for the $N^+(H_2,H)NH^+$ reaction at nearly the same energy.[20] In that case, the NH^+ scattered through large angles was much less internally excited than was the forward scattered product. In an approximate sense, the $O^+(H_2,H)OH^+$ reaction at low relative energies seems to correspond fairly closely to the results predicted by the elastic spectator model,[21] in which it is imagined that the incipient OH^+ is formed without momentum transfer to, and then is scattered elastically from, the product H. However, any firm conclusions concerning the details of the internal energy distributions are prevented by the effects of low energy and angular resolution combined with target gas motion.

While the product distributions for $O^+(H_2,H)OH^+$ are peaked in the forward direction at low relative collision

energies, this peaking is not as sharp as that which occurs in the $N_2^+(H_2,H)N_2H^+$ and $Ar^+(D_2,D)ArD^+$ reactions[12,22,23] at similar relative energies. In this particular respect, the $O^+(H_2,H)OH^+$ and $N^+(H_2,H)NH^+$ reactions are quite similar. It is not yet clear what specific features of a potential energy surface are responsible for marked forward peaking of a product angular distribution, but such distributions seem to occur for those reactions which are exoergic and in which there are relatively strong, long range attractive forces between reactants. In this respect it is of interest to note that the reactions of N_2^+ and Ar^+ with H_2 are rather more exoergic ($\Delta H \approx -1.6$eV for both) than are the reactions $O^+(H_2,H)OH^+$ and $N^+(H_2,H)NH^+$, (-0.43 and $\approx$ 0eV, respectively) for which the product distributions are less strongly forward peaked.

Figure 3 shows the OH^+ product distribution for the reaction carried out at 8.3eV initial relative energy, and Fig. 4 shows the OD^+ distribution from O^+-D_2 collisions at nearly the same relative energy. The two distributions are very similar, and clearly differ from the results obtained at lower relative energies. While the intensity distributions from the 8eV experiments are asymmetric about the $\pm$ 90° axis with most of the product forward of the center-of-mass velocity, the forward peak observed at lower energies has been replaced by a broad undulating ridge.

The reason for this change in the nature of the distribution becomes apparent when one considers the limitations imposed by energy conservation and product stability. The quantity Q may be expressed as the difference between the exoergicity of the reaction $-\Delta E_o^o$ and the product internal excitation U'. That is,

$$Q = E'_{rel} - E_{rel}$$
$$= -\Delta E_o^o - U'$$

For products in their ground electronic states, U' must lie between zero and the dissociation energy of OH^+ to $O(^3P)$ and H^+, 4.95eV. Thus Q is bounded according to

$$-\Delta E_o^o - U' \leqslant Q \leqslant -\Delta E_o^o$$

$$-4.5 \leqslant Q \leqslant 0.43\text{eV}$$

The lower limit for Q of -4.5eV arises from the necessity that $OH^+(^3\Sigma^-)$ must be stable with respect to dissociation to $O(^3P)$ and H^+ in order to be observable. The locus of this product stability limit is shown as the circle labeled Q = 4.5eV in Figs. 3 and 4.

As has been noted, the peak in the product distribution observed at low relative energies corresponds closely to product formation by the spectator stripping process. According to this model, the internal energy of the product is equal to the sum of the exoergicity of reaction $-\Delta E_o^o$, and E_a, the kinetic energy of the projectile ion

relative to the atom it abstracts. Thus

$$U'_{ss} = -\Delta E_o^o + E_a$$

$$-Q_{ss} = E_a = \frac{1}{2}\frac{AB}{A+B} v_o^2 = \frac{B}{A+B} E_L \qquad (2)$$

where A and B are the masses of the ion projectile and the abstracted atom, respectively, v_o is the initial relative speed, and E_L is the initial energy of the projectile in the laboratory system.

According to the spectator stripping model, the Q value of the intensity peak becomes more negative as the projectile energy E_L increases. Eventually, the internal energy of OH^+ formed by spectator stripping reaches the dissociation energy of the $^3\Sigma^-$ state, and Q reaches its apparent lower limit of -4.5eV. At and above the corresponding relative energy, OH^+ in the $^3\Sigma^-$ state formed by spectator stripping is no longer stable, and the forward peak must either disappear or move to velocities that are higher (and thus OH^+ internal energies that are lower) than those that correspond to the spectator stripping velocity. In Figs. 3 and 4 we see that the small cross which gives the velocity of product formed by spectator stripping lies very close to the limiting Q = -4.5eV circle. Thus the substantial decrease of the magnitude of the forward peak in the product distribution at these energies is a result of the instability of the product OH^+ or OD^+ formed in the $^3\Sigma^-$ state by spectator stripping.

This conclusion is re-enforced by the results shown in Figs. 5 and 6. In Fig. 5, the OH^+ formed by spectator stripping lies at Q = -5.3eV, a value at which $OH^+(^3\Sigma^-)$ is unstable with respect to dissociation. The peak at the stripping velocity has in fact disappeared, and the regions of maximum intensity lie at approximately $\pm 60°$. The further evolution of the distribution is shown in Fig. 6, obtained at a relative energy of 15eV. The intensity in the small angle region has fallen to a very small value, and broad intensity maxima again occur at $\pm 60°$.

It will be noted in Fig. 5 that while there is no intensity peak at the spectator stripping velocity, there is in fact a ridge of appreciable intensity at 0° and a Q value of -5.5eV. The presence of substantial intensity at values of Q less than -4.5eV seems at first to be disturbing, since OH^+ in this region must possess internal energy in excess of the amount needed to dissociate to $O(^3P)$ and H^+. There is, however, a satisfactory explanation.

We attribute the intensity ridge in the region $-6.5 < Q < -4.5$eV to formation of OH^+ in its first excited electronic state, $^1\Delta$. The location of the $^1\Delta$ state is not known experimentally, but its minimum energy has been calculated[8,9] to lie approximately 2.1eV above the $^3\Sigma^-$ ground state. The $^1\Delta$ state must dissociate to atomic

products which have a combined oribital angular momentum of $2\hbar$. The lowest lying such combination is $O(^1D)$ and H^+, which are placed 1.96eV above $O(^3P)$ and H^+. The calculations of Liu and Verhaegen[9] do in fact indicate that $OH^+(^1\Delta)$ dissociates to H^+ and $O(^1D)$. Thus the limits on Q for formation of $OH^+(^1\Delta)$ are expected to be

$$-6.5 \leqslant Q \leqslant -1.7\text{ev}$$

The broad intensity ridge at 0° in Fig. 5 does lie quite close to $Q = -5.3$eV, which suggests that this feature represents $OH^+(^1\Delta)$.

Other product intensity maps tend to confirm this interpretation. Two experiments at 10eV relative energy with D_2 as the target were performed, and in both cases a small subsidiary intensity maximum at 0° and $Q = -6.7 \pm 0.5$eV was found. Further indications of the importance of product OD^+ with $Q < -4.5$eV will be evident in Fig. 8.

Even though we find evidence for formation of the $^1\Delta$ state only when the relative collision energy is 8eV or greater, it can not be concluded that the $^1\Delta$ state is formed only in collisions in this range of relative energies. The allowed ranges of Q for the $^3\Sigma^-$ and $^1\Delta$ states overlap, and any product which appears between $Q = -1.7$ and -4.5eV could be in either state. Only for Q values outside this range can an assignment of the electronic state of the product be made with any substantial degree of certainty.

For $-1.7 \leqslant Q \leqslant 0.43$eV, the $^1\Delta$ state is inaccessible, and the product must be in the $^3\Sigma^-$ state. For $-6.5 \leqslant Q \leqslant -4.5$, only states which dissociate to $O(^1D)$ and H^+ or more highly excited atomic products are stable. For projectile energies relative to the abstracted atom of greater than 4.5eV, stable formation of the $^3\Sigma^-$ state by stripping is not possible. Therefore in this energy range (above 8eV relative energy) the small angle region is cleared of interference, and this allows the $^1\Delta$ product lying between $Q = -6.5$ and -4.5eV to be recognized. The $^1\Delta$ state may be formed in collisions at the lower initial relative energies, but can not be distinguished from the $^3\Sigma^-$ state.

Inspection of Fig. 1, the state correlation diagram, suggests a mechanism by which $OH^+(^1\Delta)$ can be formed. During collisions in which the H_2 or D_2 has its internuclear axis oblique or nearly perpendicular to the direction of the incoming O^+, the system can pass through or near the triangular conformations where the $^4A_2$ surface, which correlates with reactants $O^+(^4S)$ and $H_2(^1\Sigma)$, crosses the $^2B_2$ surface, which correlates with the products $OH^+(^1\Delta)$ and $H(^2S)$. The mixing of these two surfaces caused by spin-orbit interaction is evidently sufficient to allow a fraction of the reactants to transfer to the $^2B_2$ surface and continue to $OH^+(^1\Delta)$ and H. This same spin-orbit interaction is responsible for the small but finite

production of $O^+(^4S)$ that occurs[15] when H_2O is ionized to the $^2B_1$, $^2A_1$, and $^2B_2$ states of H_2O^+. Note that the transfer from the $^4\Sigma^-$ surface of linear OHH^+ to the $^1\Delta$ surface is unlikely, since for linear geometry, no crossings of these states occur. Moreover, there are no non-zero spin-orbit matrix elements between Σ and Δ states of a linear molecule.[10] Thus, formation of $OH^+(^1\Delta)$ is definitely to be associated with collisions which substantially depart from collinearity.

A particularly dramatic demonstration of the effect of the product stability requirement can be obtained from the study of the reaction of O^+ with HD. Figures 7 and 8 show, respectively, maps of the OH^+ and OD^+ intensities obtained from O^+-HD collisions at 6.3eV relative (40eV laboratory) energy. The OH^+ distribution is sharply forward peaked, with a maximum at the spectator stripping velocity, very much like the OH^+ from the O^+-H_2 reaction at the same laboratory energy (Fig. 2). Figure 8 shows, however, that the OD^+ from O^+-HD collisions at the same laboratory energy has intensity maxima at $\pm$ 45°, and only a somewhat lower ridge of intensity at 0°. In large measure, Fig. 8 resembles Fig. 4, the OD^+ distribution from O^+-D_2 collisions, also obtained at 40eV laboratory energy.

In Fig. 8, there is considerable product intensity at small angles in the region where $Q < -4.5$eV. We feel

that this is a further manifestation of the presence of $OD^+(^1\Delta)$.

The difference in the OH^+ and OD^+ distributions obtained from O^+-HD collisions at the same laboratory and relative energy is principally a consequence of product stability requirements. For 40eV O^+ ions, OH^+ formed by spectator stripping has a Q value of -2.3eV, or an internal excitation energy of 2.7eV, which lies well within the limit imposed by product stability. In contrast, OD^+ formed by spectator stripping from HD at this projectile energy has Q = -4.45eV, or an internal excitation of 4.9eV, almost exactly equal to the dissociation energy. When allowance is made for the spread of initial energies arising from the beam distribution and target gas motion, it is not surprising that there is a smaller production of OD^+ at small angles for this projectile energy. The striking difference between the velocity vector distributions of OH^+ and OD^+ from HD is a very convincing demonstration of the basic validity of the spectator model for <u>small angle</u> reactive scattering in this system.

The general evolution of the product distributions from H_2, D_2, and HD from forward peaked at low energies to larger angle scattering at higher collision energies is consistent with the limitations imposed on the dynamics by the product stability requirement. The grazing collisions that produce forward scattering must involve a rather weak interaction of the newly formed product OH^+ or OD^+ with the free atom. Such collisions therefore tend to leave a major

fraction of the total available energy as internal excitation of the product molecule ion, and may fail to produce stable product molecules when the initial relative energy of collision is high. Product scattered into the larger angle regions comes from collisions in which the impact parameter is small, and the interaction between all atoms is relatively strong. In such collisions there is at least the opportunity for stabilization of the product molecule. The intensity maxima at approximately $\pm 60°$ in Figs. 3, 4, 5, 6, and 8 evidently represent the most favorable compromise between large impact parameter collisions which are more probable but tend to produce unstable product, and small impact parameter collisions which are less probable, but tend to produce stable product.

It should be noted that the $O^+(H_2,H)OH^+$ reaction and its isotopic variants constitute the first example in which the forward peak has disappeared when the internal energy of the products formed by spectator stripping exceeded the dissociation energy. The reactions[12,22,23] of N_2^+, CO^+, and Ar^+ with H_2 and D_2 all show a product HX^+ peak at or near the spectator stripping velocity for fairly low relative energies. For the higher relative energies at which product formed by spectator stripping would be unstable, the forward scattered product peak is not lost, but instead moves (with diminished intensity) to higher velocities where the product molecule is stable. Thus these systems apparently possess a feature in their potential energy surfaces which is absent in the O^+-H_2

system: the feature which makes possible a forward recoil of the departing molecular ion, and which stabilizes a noticeable fraction of the product at small angles against dissociation.

It is informative to compare the ratio of the maximum intensities of OH^+ scattered at 0° and 180° for O^+-HD collisions (Fig. 7) with the same ratio for O^+-H_2 collision at the same relative velocity, or laboratory projectile energy (Fig. 2). It is seen that, relative to the forward peak intensity, less OH^+ is backscattered from HD than from H_2. A similar comparision of Figs. 4 and 8 shows that relative to the forward intensity maxima at 45°-70°, there is more OD^+ backscattered from HD than from D_2. That is, relative to the scattering from the homogeneous isotopic molecules H_2 and D_2, reactive backscattering (~180°) from HD shows an excess of OD^+ and a deficiency of OH^+.

This isotope effect for backscattering becomes even more obvious upon examination of Figs. 9 and 10, the OH^+ and OD^+ distributions from O^+-HD collisions at 11.9eV relative energy. In Fig. 9, the spectator stripping peak for OH^+ is missing for stability reasons, and the forward intensity maxima lie at ±45°. The OH^+ intensity at angles greater than 90° is very small. The deficiency of OH^+ at large angles is even more striking when one compares Fig. 9

with Fig. 3, the distribution of OH^+ from O^+-H_2 collisions at the same relative velocity.

In Fig. 10, the distribution of OD^+ from O^+-HD collisions at a laboratory energy of 75eV, the "forward" scattered intensity peaks lie at $\pm 90°$, and the intensity at angles near 180° is the same as the intensity of the small angle peaks. This is in clear contrast to the distribution in Fig. 6, which comes from O^+-D_2 collisions at the same relative velocity. In Fig. 6, the OD^+ intensity at 180° is clearly less than at the peaks located at $\pm 45°$. Thus again, relative to the small angle scattering, OD^+ from HD shows an excess intensity at 180° when compared with OD^+ from D_2.

An explanation of these isotope effects in terms of a simple kinematic model would be valuable. One particularly simple model that has been proposed in an attempt to explain hyperthermal reactions is the ideal knockout process.[24,25] In this picture, the projectile ion collides impulsively and elastically with one of the atoms of the diatomic target, and then, with its velocity correspondingly diminished, the projectile picks up the remaining atom to form the product. For this ideal process, the product is scattered through 180° in the barycentric system, and it is easy to show that the internal excitation energy of the product is

$$U' = -\Delta E_o^o + \frac{B}{A+B}\left(\frac{A-C}{A+C}\right)^2 E_L \qquad (3)$$

where E_L is the laboratory energy of the ion projectile, A is the projectile mass, B is the mass of the atom in the product, and C is the mass of the target atom first struck by the projectile.

Application of Eq. (3) shows that the ideal knockout model is quite inconsistent with our experimental findings. For 75eV O^+ colliding with HD, Eq. (3) indicates that OH^+ formed by the knockout process and appearing at 180° in the barycentric system should be stable, but OD^+ should not be. Therefore, according to the knockout model, OH^+ should be the predominant backscattered ion at this energy. This is contrary to the experimental facts. Equation (3) also indicates that OD^+ from O^+-D_2 collisions should be more stable that OD^+ from O^+-HD collisions at the same projectile energy. It thereby suggests that in the high energy regime, backscattered OD^+ should be relatively more prominent from D_2 than from HD. Again, this is contrary to the experimental findings. Finally, the indication that it is easier to form stable backscattered OH^+ from HD than from H_2 is inconsistent with our observation that backscattered OH^+ is relatively more important from H_2 than from HD. Thus the simple knockout model fails to provide explanations for the most obvious qualitative features of our experimental results. A similar failure of the model was noted[12] in connection with the N_2^+-H_2 system and its isotopic variants.

The failure of the ideal knockout model to explain the reactive backscattering is not too surprising, considering the constraints that must be satisfied in order for such a process to take place. If the atom struck initially by the projectile is to be ejected without encountering the second target atom, the target diatomic molecule must be oriented nearly perpendicularly to the velocity vector of the projectile, and the impact parameter must be restricted to a small range of values. Also, the initially struck atom must move away from the collision region without experiencing any bonding or long range forces from either the projectile or its partner in the target atom. In view of the nearly symmetric configuration implied by approach of the projectile perpendicular to the axis of the target, the extreme difference in the forces on the two atoms of the target which is implicit in the ideal knockout model seems very unlikely. Failure of this simple "perpendicular collision" model and recognition of the fact that the lowest energy regions of the quartet surface for O^+-H_2 are those in which the atoms are collinear, both suggest that to understand the behavior in the intermediate range of collision energies, consideration of a collinear collision model would be profitable.

As is well known, the dynamics of a collision process can be discussed most simply in terms of coordinates which lead to an expression for the kinetic energy containing

no cross terms. For the reaction A(BC,C)AB restricted to collinear geometry, we can choose y, the BC internuclear separation, and x, the distance between A and the center of mass of BC as our coordinates, and the kinetic energy becomes

$$T = \frac{1}{2}\frac{A(B+C)}{M}\dot{x}^2 + \frac{BC}{B+C}\dot{y}^2$$

where M is the total mass of the system. However, a further simplification is introduced if we further transform to

$$X = x \qquad y = aY$$

and choose the constant a so that the coefficients of $\dot{X}^2$ and $\dot{Y}^2$ in the kinetic energy expression will be the same. This gives

$$T = \frac{1}{2}\frac{A(B+C)}{M}(\dot{X}^2 + \dot{Y}^2)$$

where

$$X = r_{AB} + \frac{C}{B+C} r_{BC}$$

$$Y = r_{BC}/a$$

$$a^2 = \frac{A(B+C)^2}{BCM}$$

and r_{AB}, r_{BC} are respectively the AB and BC internuclear distances. The coordinates X, Y were introduced by Eyring and Polanyi[26] in connection with molecular collision dynamics. When they are used, a frictionless mass point sliding on a potential energy surface will correctly represent the actual dynamics of a three atom collinear collision. The X, Y

coordinates are very closely related to those used by Smith[27] in his discussion of product excitation in exoergic reactions, and are one of a class of coordinates recently discussed by Hirschfelder[28] in connection with isotope effects in chemical reactions.

When plotted in terms of the X, Y coordinates the potential energy surface for the collinear A(BC,C)AB reaction assumes a "skewed" form. That is, the angle β between the equipotential contours in the asymptotic exit valley (r_{AB} = const) and those in the entrance valley (r_{BC} = const) is less than 90°, and is given by

$$\tan^2\beta = \frac{BM}{AC}$$

Thus the reaction coordinate turns through the angle $\pi-\beta$ as the system passes from reactants to products. In order for reaction to occur, the potential energy surface must be shaped so that the forces exerted on the representative mass point allows it to turn the corner from the reactant valley to the product valley.

It is clear that for a reaction such as O^+ with HD, the angle β will be small (37.6°) when O^+ attacks the H atom (O^+-HD), and larger (57.0°) when the D atom is being attacked (O^+-DH). For reaction of O^+ with H_2 or D_2, β will have the intermediate values of 46.7° and 48.2°, respectively. Figure 11 shows this effect schematically for a hypothetical surface of the type that might apply to the collinear O^+-H_2 system.

For collisions of energy less than 1eV, the trajectories will be strongly influenced by the details of the shape of the potential energy surface near the minimum energy path, and the effects of varying β will be difficult to discern. However, for collisions of higher relative energy, the trajectories will be increasingly influenced by the nature of the shape of the repulsive walls of the potential energy surface. At these higher energies, the true surface increasingly resembles in its region of small internuclear separations, a surface which represents the interaction of ideal hard spheres. In this case, the two repulsive walls are infinitely steep, and intersect each other with the interior angle β. Thus, while we do not propose that in the range of 3-12eV the true potential energy surface for O^+-H_2 can be accurately represented by the ideal hard sphere surface at small internuclear separations, it seems clear that the approximation may be close enough at the higher energies so that an analysis of the hard sphere case will reveal some of the experimentally observed isotope effects.

For ideal collinear hard sphere collisions[28] with $\beta = 60°$ (approximately the O^+-DH case), the projectile A hits the first target atom B, B hits C, then AB moves away as product with zero internal energy. For $\beta = 45°$ (nearly the O^+-H_2 and O^+-D_2 cases), a sequence of three hard sphere

collisions (A,B; B,C; A,B) reflect the particles back out the reactant channel. For $\beta = 36°$ (the O^+-HD case) the product channel is again reached, but only after four hard sphere collisions. This analysis would suggest substantial reaction probability for O^+-DH and D^+-HD, but not for O^+-H_2 and O^+-D_2. However, there are three difficulties with this conclusion.

First, nearly collinear collisions are much more likely than exactly collinear ones, and in the non-collinear case, a sequence of four hard sphere collisions is very unlikely. The failure of the complete sequence of four collisions to occur would significantly lower the expected yield of backscattered OH^+ from O^+-HD relative to the OD^+ yield from O^+-DH. Second, if one approaches the real potential by softening the hard sphere forces, the repulsive walls at the end of the reactant valley become curved, and any equipotential contour has a range of slopes with respect to the reactant channel axis. In general this leads to effective values of β which are greater than those computed from the mass factors alone, and this alteration might suggest an increased reaction probability for the O^+-H_2 and O^+-D_2 cases. Finally, it should be recognized that in a collision in which the conditions for the impulse approximation are nearly satisfied, it is the energy of the projectile relative to the atom it strikes, rather than the energy

relative to the whole molecule which is of greatest significance.[29] This means that for a particular projectile laboratory energy, the hard sphere analysis may be a better approximation for O^+-DH than for O^+-HD. In the latter case, the more nearly vibrationally adiabatic motion can be expected to lower the reaction probability. Thus, the hard sphere analysis combined with the qualifications necessarily imposed by real potential energy surfaces seems to lead to qualitative conclusions which are consistent with the observed isotope effects.

Similar isotope effects have been observed experimentally in the N_2^+-HD system[12] at moderate energies (< 8eV) and in the O_2^+-HD system at collision energies high enough so that the reaction proceeds by direct interaction.[30] Also, in a recent study of the ^{18}F+HD reaction by classical trajectories on a semi-empirical potential surface, Muckerman[31] observed an isotope effect in the total cross section favoring DF by approximately 50% in the 1-6eV range of relative energy. Moreover, the propensity for formation of DF over HF was greatest in the large angle region for collisions of 1eV and 5eV relative energy.

The similarity of the large angle isotope effects in systems of such different chemical nature suggests that they have their origin in the mass combinations, and are influenced to a secondary degree by the details of the

potential energy surfaces. If the surface is such that as A approaches, a strong repulsion between B and C builds up, then the system will tend to pass easily into the product valley. Thus in these circumstances, the differential reaction cross section for backscattering will be large, and the isotope effect favoring abstraction of D from HD will tend to be small. In contrast, if the potential energy surface is of a type where A can interact repulsively with B before any appreciable BC repulsion occurs, then the slopes of the equipotential contours that are encountered by the representative mass point as it reaches the end of the reactant valley are nearly equal to the angle β. Depending on the value of β, the representative point may pass into the product channel ($\beta \approx 60°$) or be reflected back into the reactant channel ($\beta \lesssim 45°$). Thus such a surface could lead to small reactive cross sections, and a large isotope effect favoring abstraction of D from HD. The magnitudes of the experimentally observed isotope effects suggest that N_2^+-HD has a surface close to the first described, while O_2^+-HD and O^+-HD are of the more impulsive type. In fact, in a subsequent paper we will show that an impulse model which allows for other than collinear collisions provides a very satisfactory description of the O^+-H_2 reaction and its isotopic variants at higher energy.

SUMMARY

We have examined the product velocity vector distribution for the reaction $O^+(H_2,H)OH^+$ and its isotopic variations for a range of initial relative kinetic energies. The reaction proceeds from ground state reactants to products predominately in the electronic ground state via a direct interaction in which spectator stripping is a prominent feature. At the higher energies (> 8eV), the spectator stripping peak is lost when the vibrational and rotational energy of $OH^+(^3\Sigma^-)$ makes it unstable with respect to dissociation to $O(^3P)$ and H^+. However, in this energy range there is evidence for production of OH^+ in electronic states such as $^1\Delta$ that can only dissociate to excited atomic fragments, and consequently are of greater stability than the ground electronic state. Production of $OH^+(^1\Delta)$ is consistent with coupling by spin-orbit interaction of the initial $^4A_2$ surface and the $^2B_2$ surface appropriate for O^+-H_2 collisions in near C_{2v} geometry. It is particularly evident at the higher energies that OH^+ from HD is predominately scattered into the small angle (< 90°) region, while the OD^+ appears at large angles (> 90°). The propensity for formation of OD^+ at large angles can be understood in terms of the general appearance of the potential energy plotted in a coordinate system which diagonalizes the kinetic energy.

Acknowledgement: This work was supported by the U. S. Atomic Energy Commission. K. T. G. acknowledges financial support from the Miller Institute for Basic Research, and J. S. W. acknowledges pre-doctoral fellowship support from the National Science Foundation.

REFERENCES

1. F. C. Fehsenfeld, A. L. Schmeltekopf, and E. E. Ferguson, J. Chem. Phys. 46, 2802 (1967).
2. J. L. Franklin et al., Natl. Std. Ref. Data Ser. Natl. Bur. Std. (U.S.), 26, (1969).
3. B. H. Mahan, J. Chem. Phys. 55, 1436 (1971).
4. T. Fiquet-Fayard and P. M. Guyon, Mol. Phys. 11, (1966).
5. For a discussion of the electronic states and absorption spectra of H_2O, see C. R. Claydon, G. A. Segal, and H. S. Taylor, J. Chem. Phys. 54, 3799 (1971).
6. D. W. Turner, C. Baker, A. D. Baker, and C. R. Brundle, Molecular Photoelectron Spectroscopy (Wiley-Interscience, New York. 1970) p. 77.
7. G. Herzberg, Molecular Spectra and Molecular Structure I. Spectra of Diatomic Molecules, (Van Nostrand, New York, 1950) p. 561.
8. P. E. Cade, Can. J. Phys. 46, 1989 (1968).
9. H. P. D. Liu and G. Verhaegen, Int. J. Quantum Chem. 5, 103 (1971).
10. D. S. McClure, J. Chem. Phys. 17, 665 (1949).
11. H. Eyring, J. Walter, and G. E. Kimball, Quantum Chemistry (Wiley, New York, 1944) p. 326.
12. W. R. Gentry, E. A. Gislason, B. H. Mahan, and C. W. Tsao, J. Chem. Phys. 49, 3058 (1968).
13. M. H. Chiang, E. A. Gislason, B. H. Mahan, C. W. Tsao, and A. S. Werner, J. Phys. Chem. 75, 1426 (1971).

14. B. R. Turner, J. A. Rutherford, and D. M. J. Compton, J. Chem. Phys. 48, 1602 (1968).

15. B. M. Hughes and T. O. Tiernan, J. Chem. Phys. 55, 3419 (1971).

16. H. H. Harris and J. J. Leventhal, private communication.

17. W. B. Miller, S. A. Safron, and D. R. Herschback, Disc. Faraday Soc. 44, 108 (1967).

18. E. A. Gislason, B. H. Mahan, C. W. Tsao, and A. S. Werner, J. Chem. Phys. 50, 5418 (1969).

19. J. M. Parson and Y. T. Lee, J. Chem. Phys. 56, 4658 (1972).

20. E. A. Gislason, B. H. Mahan, C. W. Tsao, and A. S. Werner, J. Chem. Phys. 54, 3897 (1971).

21. D. R. Herschbach, Appl. Opt. Suppl. 2, 128 (1965).

22. K. Lacmann and A. Henglein, Ber. Bunsenges. Physik. Chem. 69, 292 (1965).

23. M. Chiang, E. A. Gislason, B. H. Mahan, C. W. Tsao, and A. S. Werner, J. Chem. Phys. 52, 2698 (1970).

24. R. J. Cross, Jr. and R. Wolfgang, J. Chem. Phys. 35, 2002 (1961).

25. J. C. Light and J. Horrocks, Proc. Phys. Soc. (London) 84, 527 (1964).

26. H. Eyring and M. Polanyi, Z. Physik. Chem. B12, 279 (1931).

27. F. T. Smith, J. Chem. Phys. 31, 1352 (1959).

28. J. O. Hirschfelder, Int. J. Quantum Chem. 35, 17 (1969).

29. B. H. Mahan, J. Chem. Phys. 52, 5221 (1970).

30. M. H. Chiang, B. H. Mahan, C. W. Tsao, and A. S. Werner, J. Chem. Phys. 53, 3752 (1970).

31. J. T. Muckerman, J. Chem. Phys. 57, 3388 (1972).

Figure Captions

Fig. 1. A partial correlation diagram for the electronic states of the H_2O^+ system. Starting from the left of the diagram, O^+ (or O) approaches H_2 (or H_2^+) along the perpendicular bisector of the H-H axis, and the system passes to products through an HOH^+ intermediate. Starting from the right side, reactants pass to products through collinear conformations. The heavy lines indicate states whose energies are known to ± 0.1eV or better.

Fig. 2. A contour map of the specific intensity $\bar{I}$ of OH^+ from O^+-H_2 collisions at an initial relative energy of 4.5eV. The radial coordinate is the speed of OH^+ relative to the center of mass of the system, and the angular coordinate is the barycentric scattering angle measured from the direction of the O^+ projectile. The small cross locates the velocity of OH^+ formed by spectator stripping. The map shows the intensity of OH^+ strongly peaked in the forward or small angle region.

Fig. 3. A contour map of the specific intensity of OH^+ formed from O^+ and H_2 after collisions of 8.3eV relative energy. The circle labeled Q = -4.5eV is the locus of OH^+ formed with an internal excitation equal to the dissociation energy of the $^3\Sigma^-$ ground electronic state.

Note the broad (in angle) ridge of intensity in the forward hemisphere ($|\theta| < 90°$), which contrasts with the sharp forward peak of Fig. 2.

Fig. 4. A contour map of the specific intensity of OD^+ from O^+-D_2 collisions at 8.0eV relative energy. Note the general resemblance to Fig. 3, and also that the peak at 0° extends into the region where $Q < -4.5$eV. This suggests formation of electronically excited states of OD^+ that dissociate to excited atomic fragments. (see text)

Fig. 5. A contour map of the specific intensity of OH^+ formed from O^+-H_2 collisions with an initial relative energy of 10.0eV. Note that the spectator stripping velocity (marked by a cross) lies between $Q = -4.5$eV, the stability limit for $OH^+(^3\Sigma^-)$, and $Q = -6.5$eV, the stability limit for $OH^+(^1\Delta)$. The intensity maxima at $\pm 60°$ lie in the region where $OH^+(^3\Sigma^-)$ is stable, but at small angles there is considerable intensity in the region between $Q = -4.5$eV and $Q = -6.5$eV, where $OH^+(^1\Delta)$ is stable, but the $^3\Sigma^-$ state is not.

Fig. 6. A contour map of the specific intensity of OD^+ formed from O^+-D_2 collisions with an initial relative energy of 15.0eV. Note the virtually complete absence

of intensity at 0°. Both $OD^+(^3\Sigma^-)$ and $OD^+(^1\Delta)$ would be unstable with respect to dissociation if they were formed by spectator stripping at these energies.

Fig. 7. A contour map of the specific intensity of OH^+ formed from O^+-HD collisions with an initial relative energy of 6.32eV. Note that the intensity maximum coincides with the spectator stripping velocity. Note also the rather small intensity in the large angle (~180°) region.

Fig. 8. A contour map of the specific intensity of OD^+ from O^+-HD collisions with a relative energy of 6.3eV. Note that in contrast with Fig. 7, there is no intensity peak at the spectator stripping velocity. Also, there is considerable intensity inside the Q = -4.5eV circle, where $OD^+(^1\Delta)$ but not $OD^+(^3\Sigma^-)$ is stable.

Fig. 9. A contour map of the specific intensity of OH^+ from O^+-HD collisions with an initial relative energy of 11.9eV. Note the very low intensity at angles larger than 90°, the complete absence of a spectator stripping angular peak, and the noticeable intensity in the $Q < -4.5$eV region at small angles.

Fig. 10. A contour map of the specific intensity of OD^+ from O^+-HD collisions at 11.9eV. Compare this with Fig. 9. Note the low intensity in the small angle region, and the nearly uniform ridge of intensity in the large angle region.

Fig. 11. A demonstration of how a hypothetical potential energy surface of the LEPS type changes when it is plotted for various isotopic combinations in terms of the coordinates X,Y which reduce the 3-particle collinear collision problem to a one particle problem. The energies are given in electron volts relative to the separated atoms, and the contours in each panel correspond to those in the upper left-hand panel. Note that the low energy contours in the region of the corner have no simple or clear relation to the angle β at which the bond distance coordinates are skewed. However, in the repulsive region, the contours tend to approximate two lines which intersect at the angle β as the energy of the contour is increased.

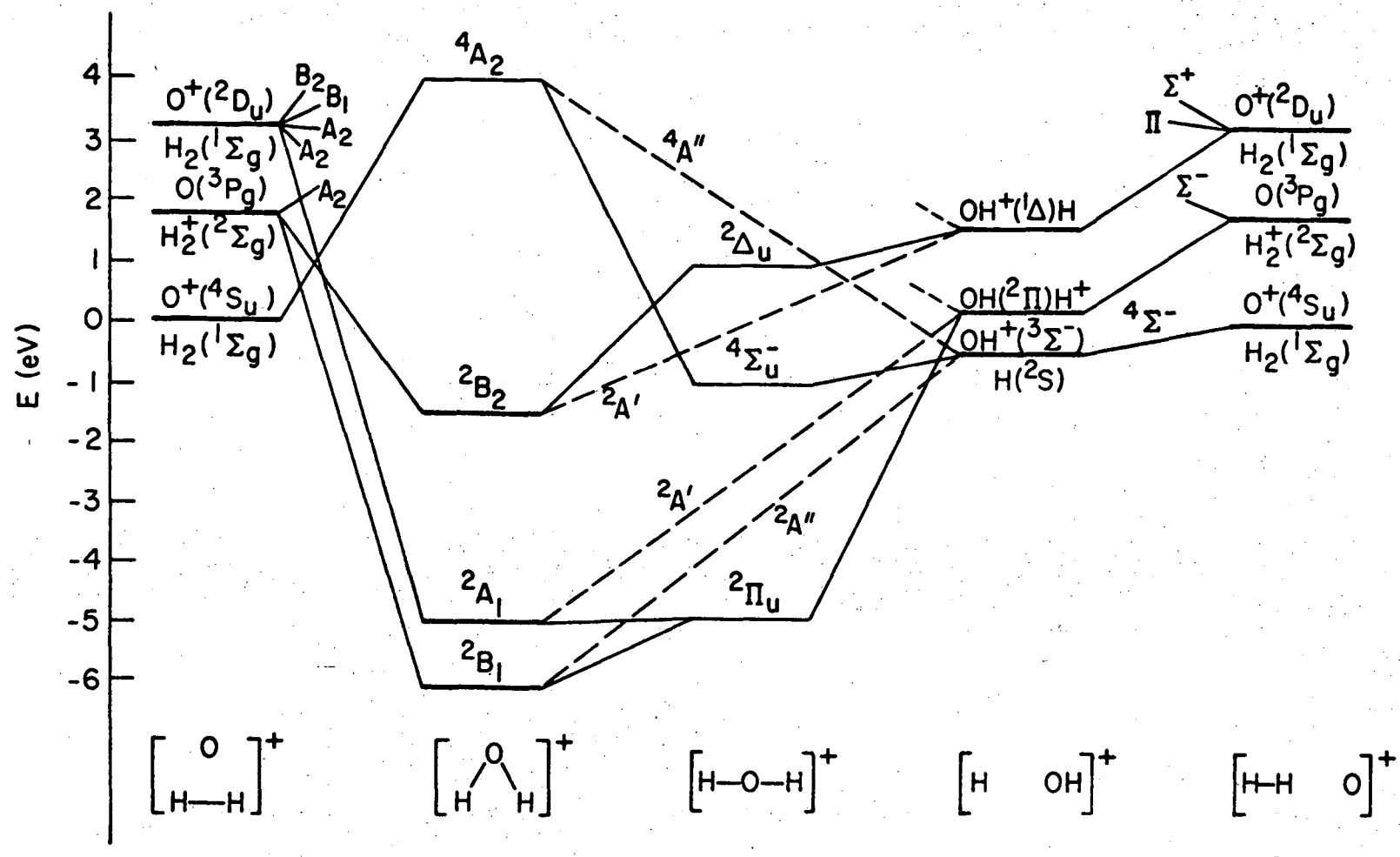
E (eV)
4
3
2
1
0
-1
-2
-3
-4
-5
-6
O+(2Du)
H2(1Σg)
O(3Pg)
H2+(2Σg)
O+(4Su)
H2(1Σg)
B2
B1
A2
A2
A2
4A2
2B2
2A1
2B1
4A″
2Δu
4Σu-
2A′
2A′
2A″
2Πu
OH+(1Δ)H
OH(2Π)H+
OH+(3Σ-)
H(2S)
Σ+
Π
Σ-
4Σ-
O+(2Du)
H2(1Σg)
O(3Pg)
H2+(2Σg)
O+(4Su)
H2(1Σg)
[O H—H]+
[O H H]+
[H—O—H]+
[H OH]+
[H—H O]+
XBL 728-6806

Fig. 1

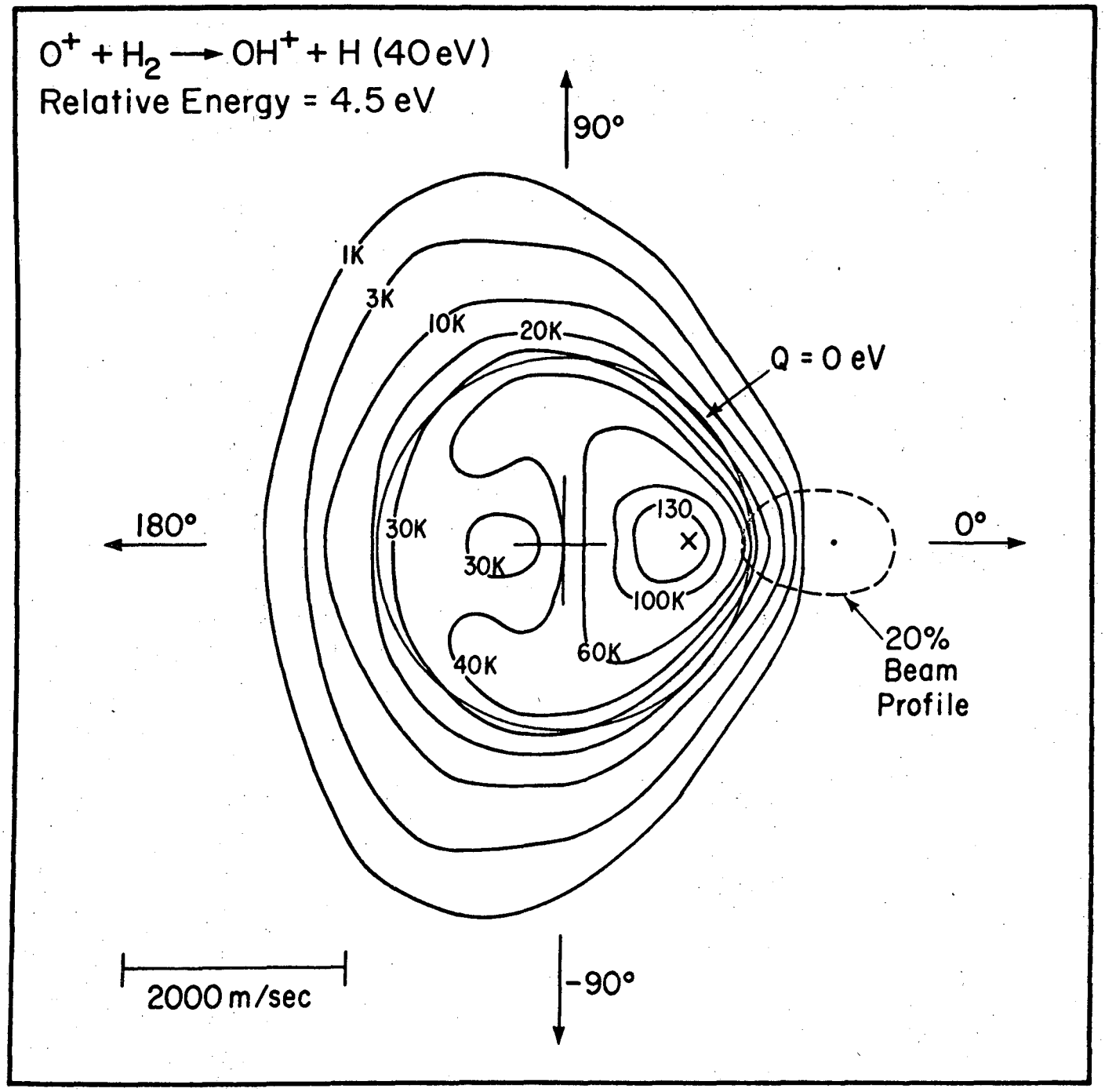

XBL727-6542

Fig. 2

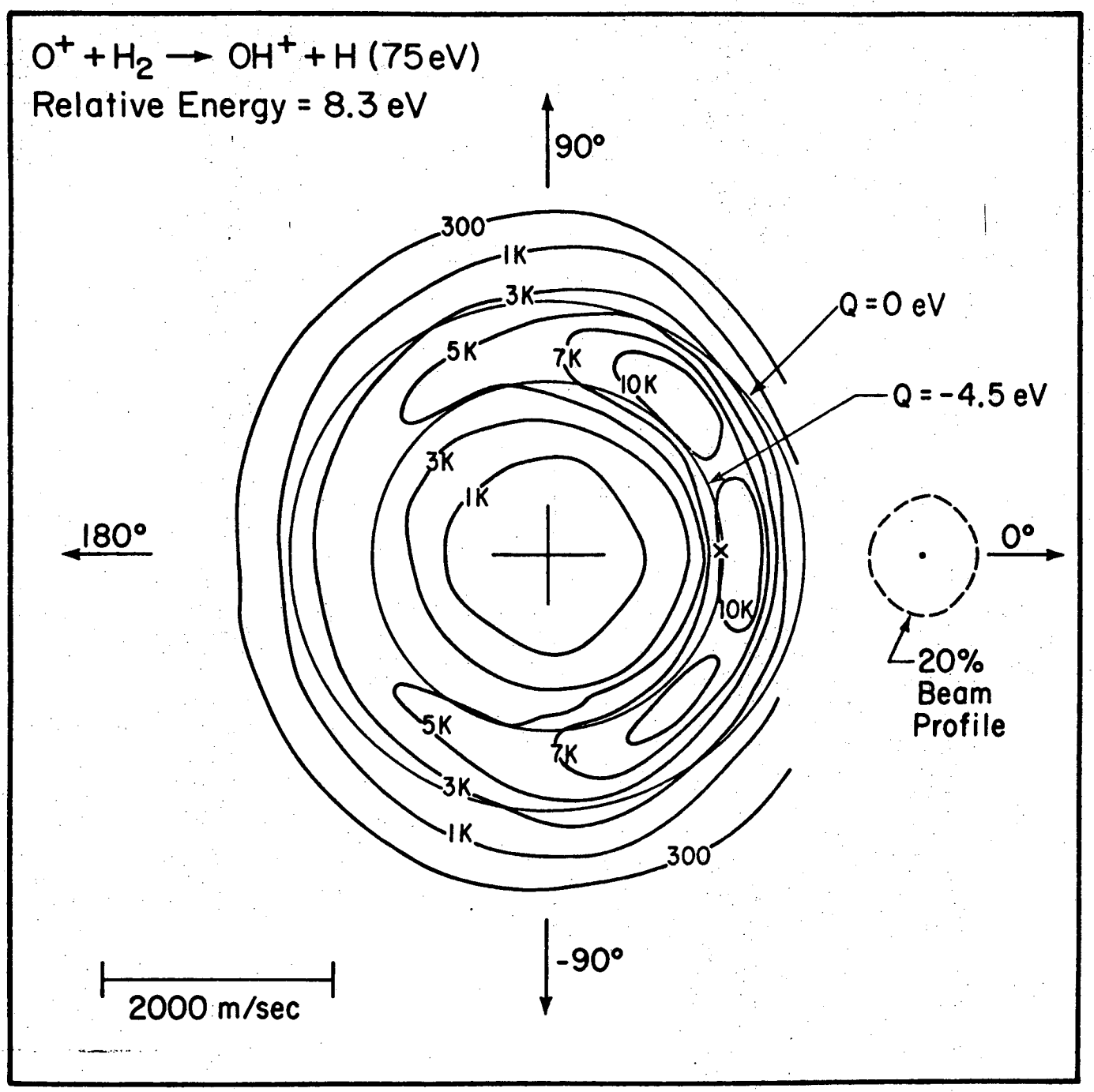

XBL 727-6535

Fig. 3

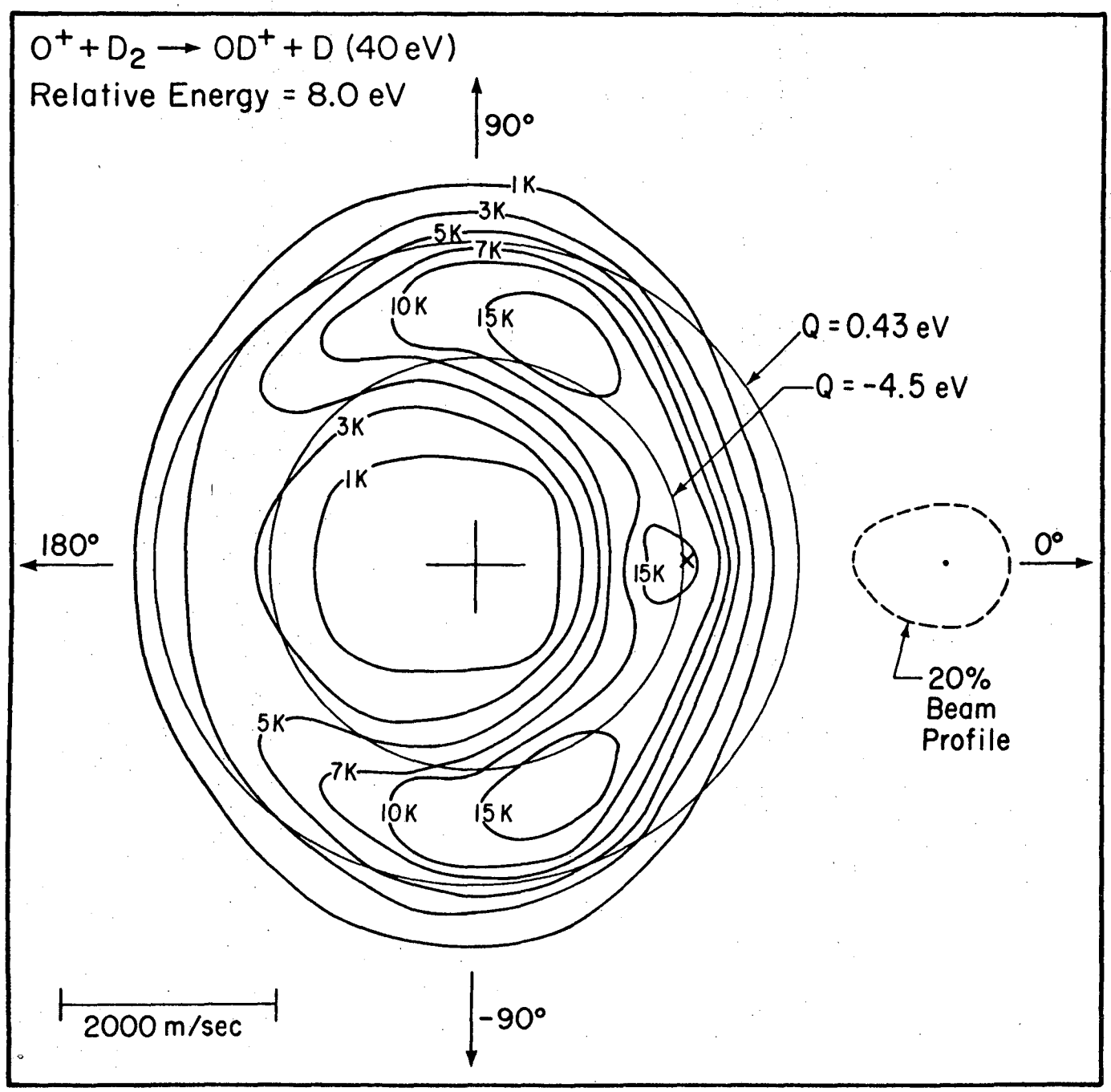

XBL 727-6534

Fig. 4

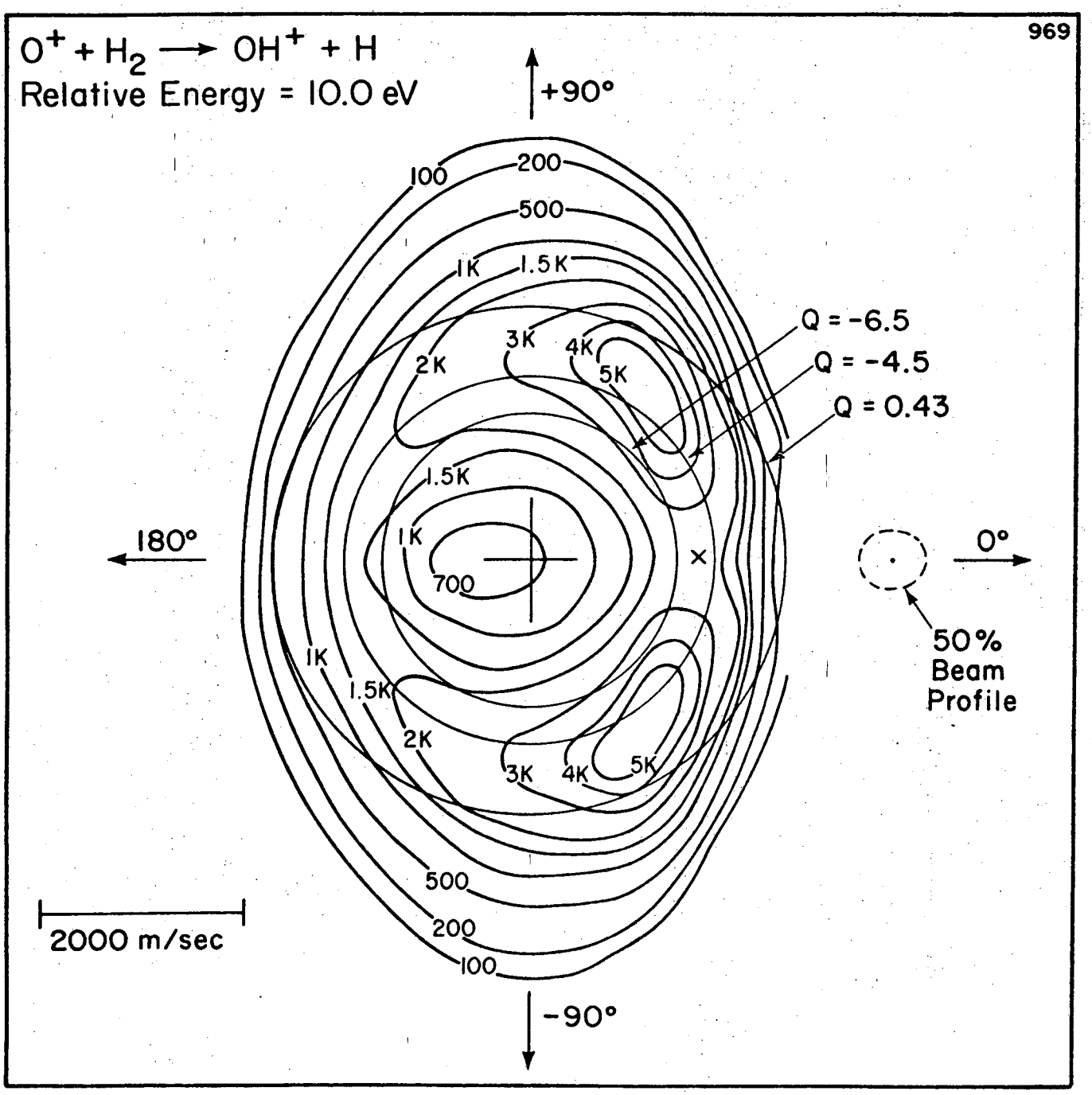
969
$O^+ + H_2 \longrightarrow OH^+ + H$
Relative Energy = 10.0 eV
+90°
-90°
180°
0°
100
200
500
1K
1.5K
2K
3K
4K
5K
700
Q = -6.5
Q = -4.5
Q = 0.43
50% Beam Profile
2000 m/sec

Fig. 5

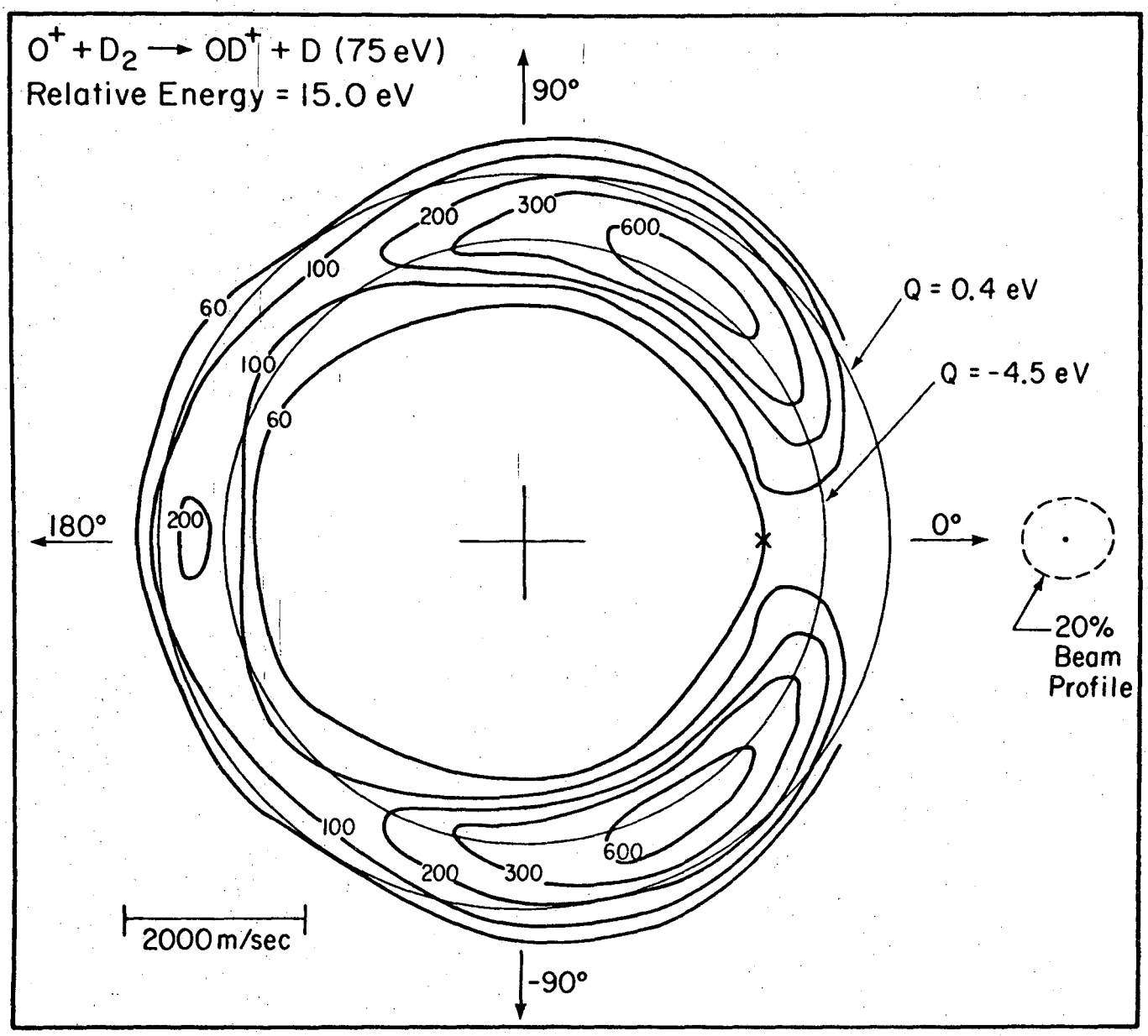

XBL 727-6544

Fig. 6

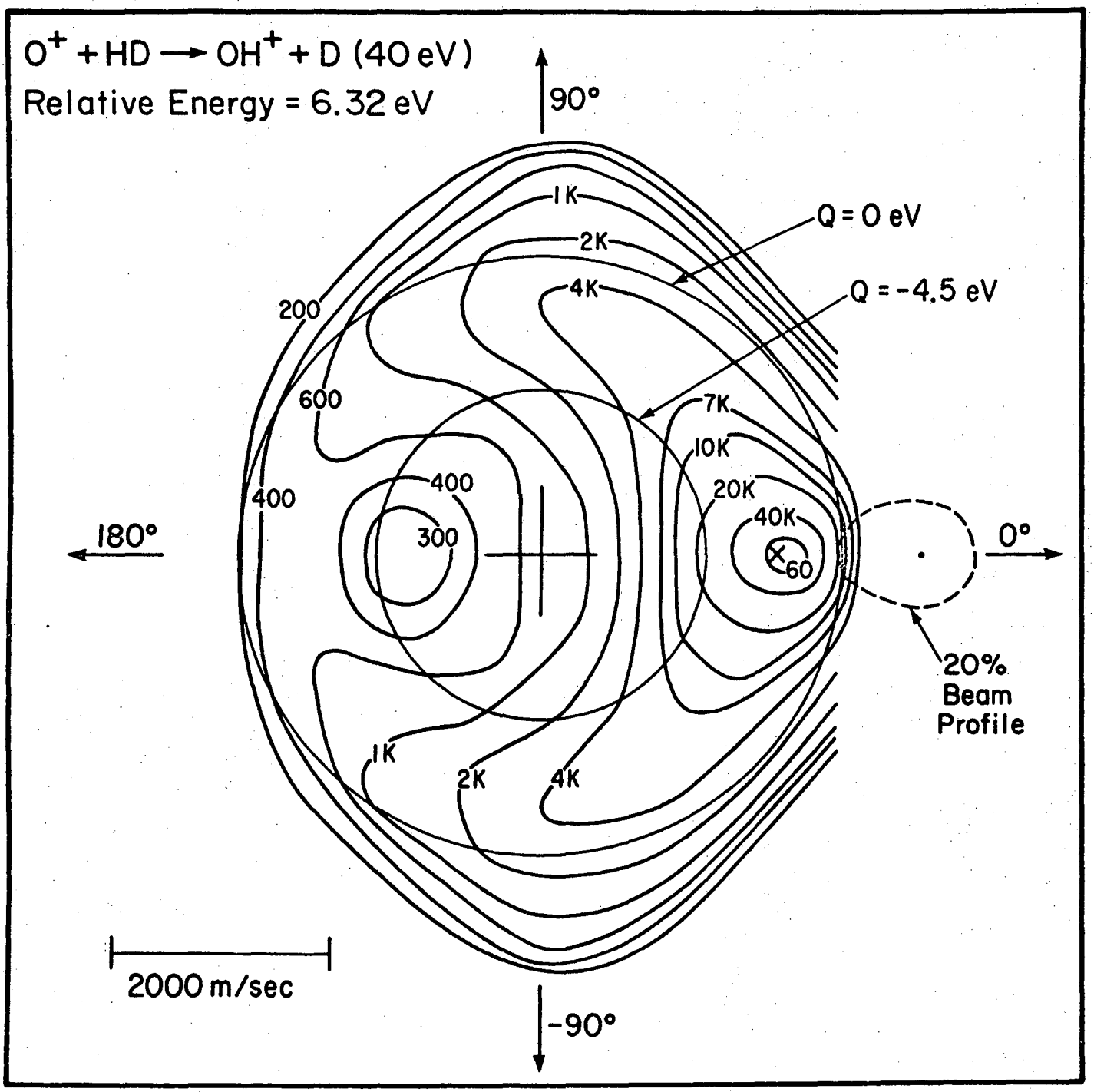

XBL 727-6540

Fig. 7

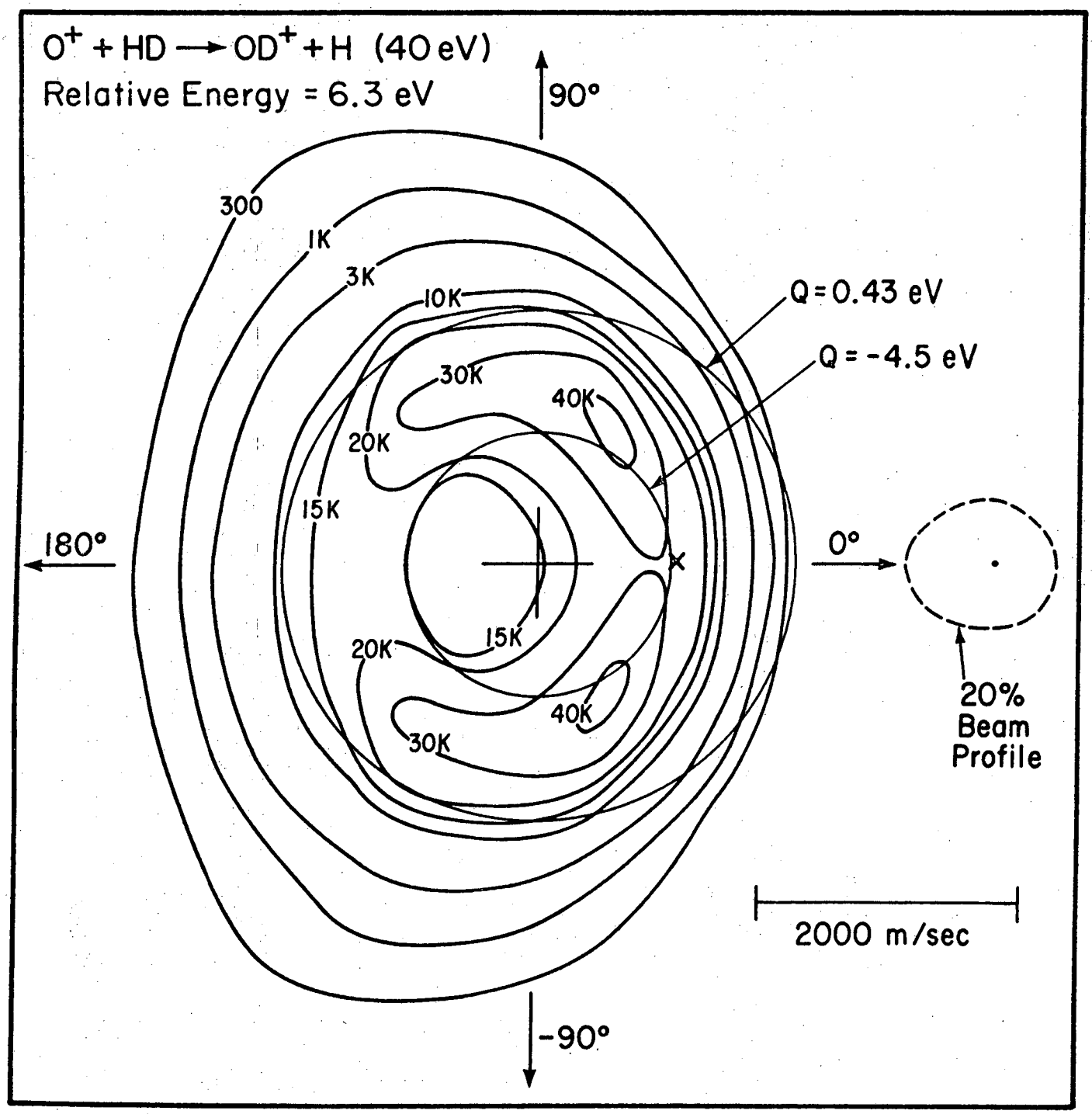

XBL727-6539

Fig. 8

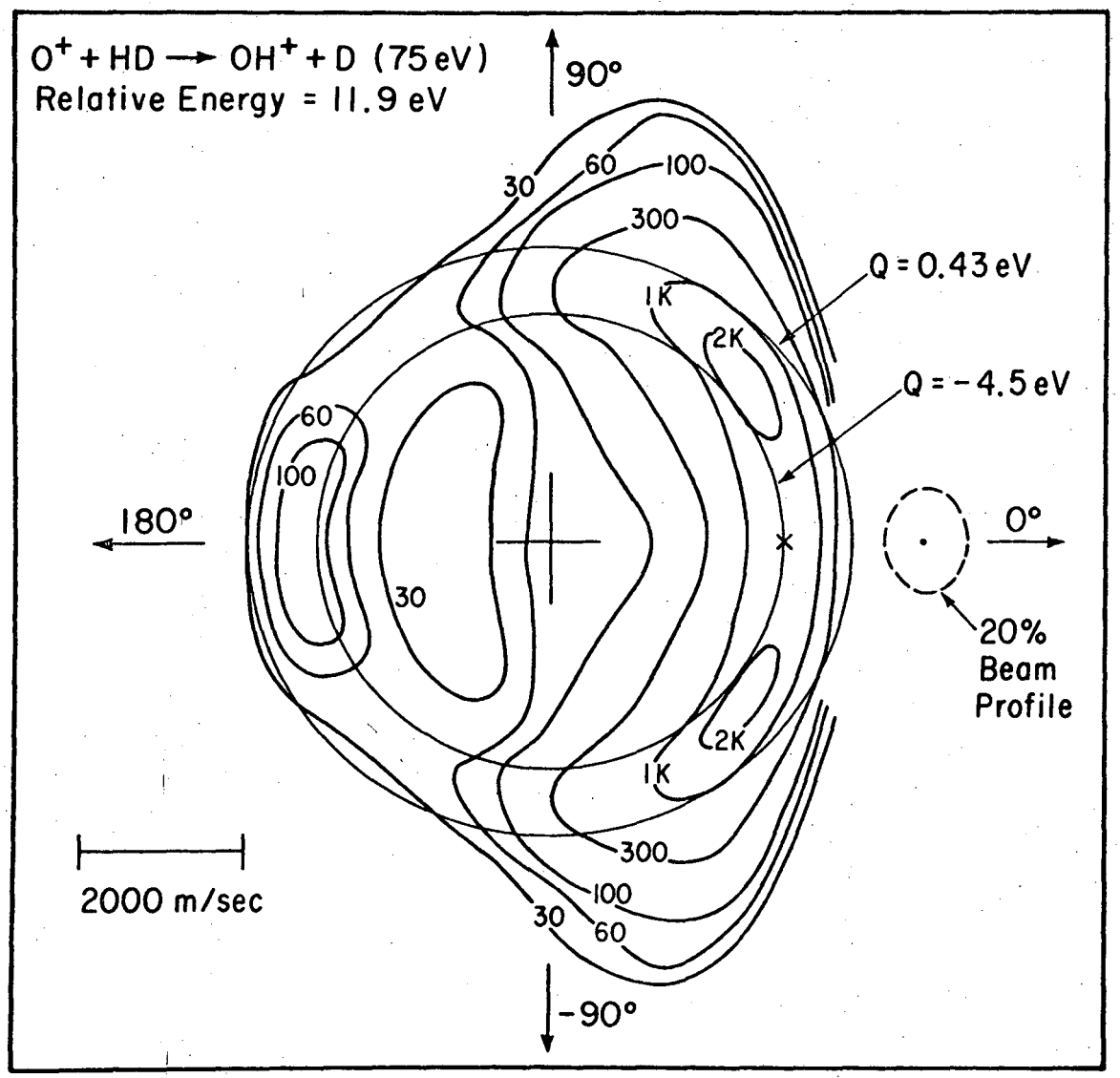

XBL 727-6588

Fig. 9

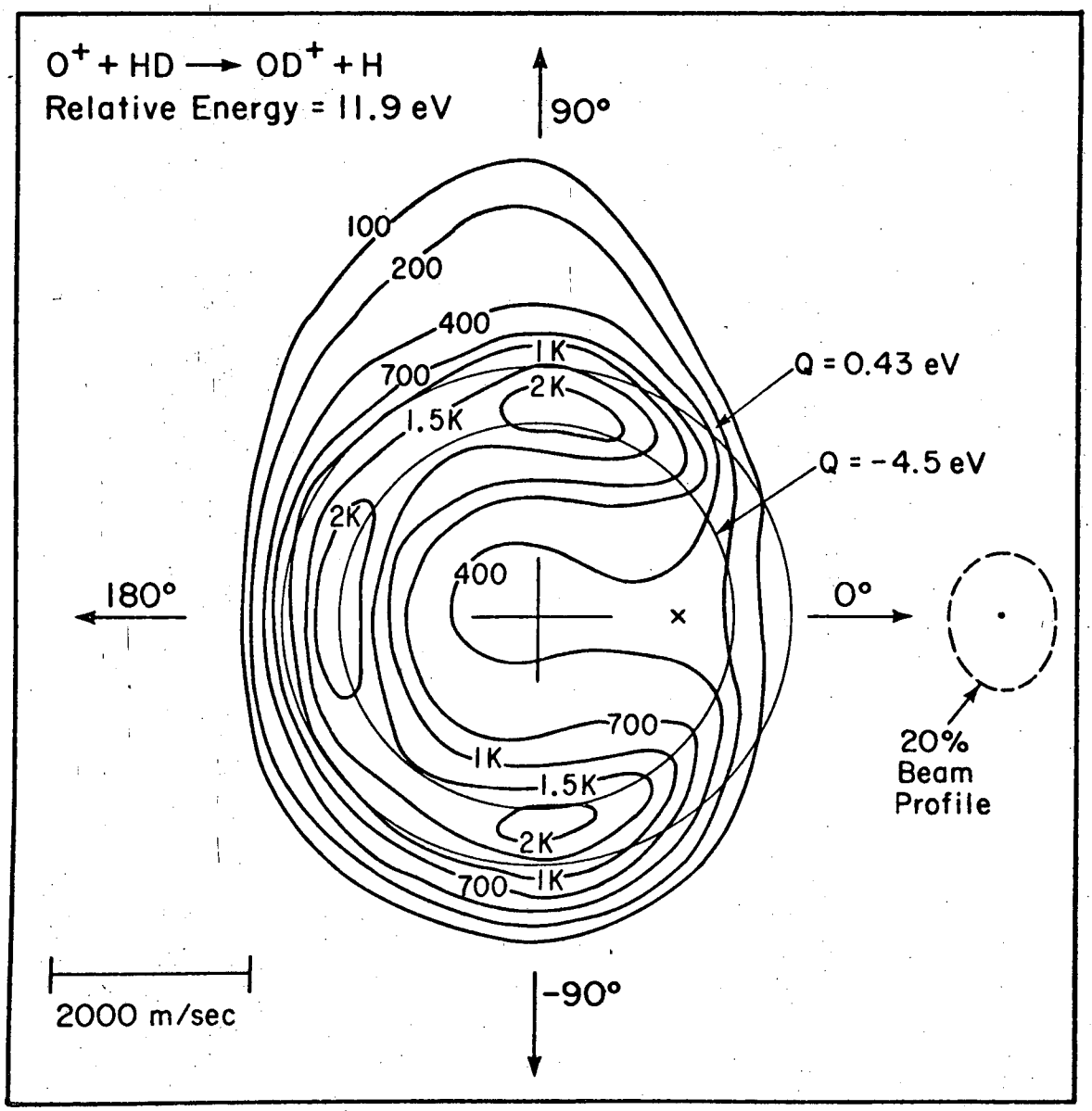

XBL727-6593

Fig. 10

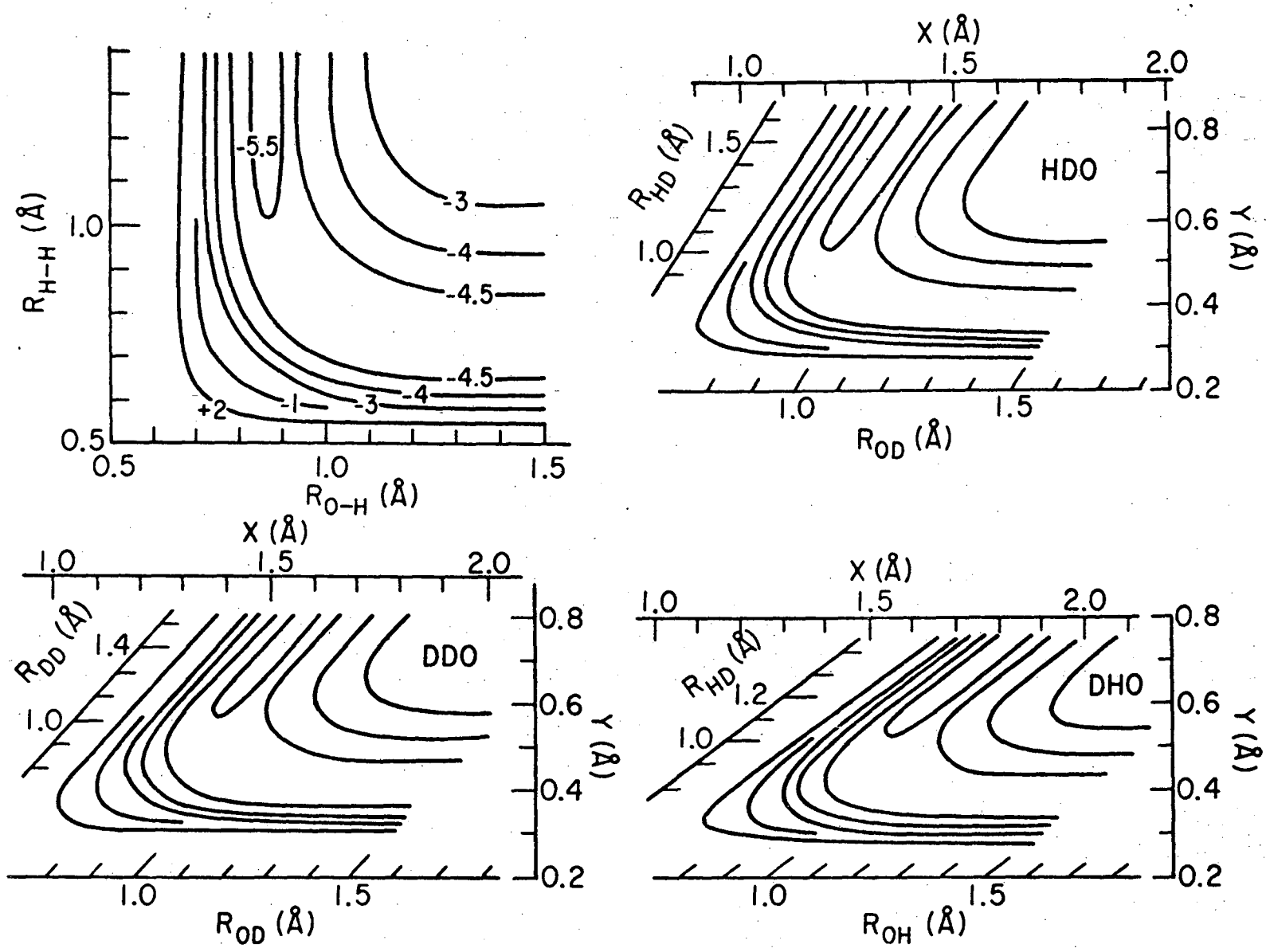
R_{H-H} (Å)
R_{O-H} (Å)
-5.5
-3
-4
-4.5
-4.5
-4
-3
-1
+2
HDO
R_{HD} (Å)
R_{OD} (Å)
X (Å)
Y (Å)
DDO
R_{DD} (Å)
R_{OD} (Å)
DHO
R_{HD} (Å)
R_{OH} (Å)

Fig. 11

LEGAL NOTICE

This report was prepared as an account of work sponsored by the United States Government. Neither the United States nor the United States Atomic Energy Commission, nor any of their employees, nor any of their contractors, subcontractors, or their employees, makes any warranty, express or implied, or assumes any legal liability or responsibility for the accuracy, completeness or usefulness of any information, apparatus, product or process disclosed, or represents that its use would not infringe privately owned rights.

TECHNICAL INFORMATION DIVISION
LAWRENCE BERKELEY LABORATORY
UNIVERSITY OF CALIFORNIA
BERKELEY, CALIFORNIA 94720